

Induced voltage at two poles of 10kV parallel distribution line caused by direct lightning strike on the phase wire of adjacent line

Yating Zhao, Jianguo Wang*, Li Cai, Quanxin Li, Mi Zhou, Rui Su, Zhiling Xu, Yadong Fan

School of Electrical Engineering and Automation, Wuhan University, Wuhan 430072, China



ARTICLE INFO

Keywords:

Induced voltage
Direct lightning
Rocket-triggered lightning
Distribution line

ABSTRACT

Triggered lightning was used to strike different phase wires of a 10 kV double circuit distribution line in 2018. The induced voltage on two poles of the other circuit is analyzed. When it struck on phase A, for the pole close to the strike point, the induced voltage of the lowest phase C is different from that of the two phases, with three obvious negative pulses and one prominent positive pulse. The negative peak of three-phase overvoltage ranges from -11.7 kV to -65.2 kV corresponding to lightning current from -8.3 kA to -18.1 kA. For the three-phase voltage on the pole far away from the strike point, its negative peak is between -10.5 kV and -42.8 kV corresponding to lightning current from -8.3 kA to -26.7 kA. The test method and results proposed in this paper will be helpful to the research on the lightning overvoltage response of parallel power distribution lines.

1. Introduction

Most distribution line failures are caused by lightning incidents, including direct and indirect strokes. Although direct stroke is not often seen compared to indirect stroke, it can cause a much higher frequency of lightning faults [1]. There are many measures to protect distribution lines, like surge arresters and ground wires. The Research about these facilities can be found in [2, 3].

There has been much research on natural lightning observation. Rosa et al. [4] concluded that the waveform and the polarity of induced voltage were highly dependent on the strike point. Short et al. [5] studied the effect of different arrester spacings on the protection of distribution lines through three years of monitoring, and it was concluded that for the line equipped with arrester at each pole, its performance was not improved, which was very strange. From 1996 to 2006, the Tokyo Electrical Power Company conducted the observation of natural lightning strikes on 6.6 kV distribution lines, and five direct lightning examples were analyzed [6]. Cai et al. [7] observed 12 flashes with 36 return strokes on a 220 V distribution line. The induced voltage was from 0.2 kV to 3.9 kV, and double-peak oscillation was observed in the waveform. Eriksson [8] reported direct natural lightning on an 11 kV distribution line, which only accounted for 4% of the total, while the recent report of natural direct lightning can be found in [9].

Except for observations of natural lightning, different methods are also taken to test the line response to lightning, like rocket-triggered

lightning, artificial lightning current injection by impulse current generator [10, 11], and scale model [12–14]. Since Newman et al. [15] triggered 17 cloud-vessel lightning flashes successfully in 1967, this technology came into research. Triggered lightning experiments were mainly carried out in America, Japan, China, Brazil, etc. since the 1990s. Barker conducted triggered lightning 145 m away from a 682 m distribution line and found that the induced voltage was the highest at the middle of the line [16]. Rubinstein et al. [17] carried out triggered lightning 20 m away from a 448 m distribution line, and oscillation waveform and impulse waveform were concluded. There are also some experiments on the difference between natural lightning and artificial lightning. Matsumoto et al. [18] measured the surges caused by natural and triggered lightning on a double circuit, 2.2 km transmission line in 1996. It was found that the natural lightning current was much larger than the triggered lightning current and the current in the arrester of phase A was only 3 kA, proving the effectiveness of line protection. In 1998, Motoyama et al. [19] analyzed multiphase back flashover caused by natural lightning on the same line.

As for direct triggered lightning, Fernandez et al. [20] used triggered lightning technology to directly hit the phase conductor on a 730 m distribution line. The performance of the arrester was demonstrated, including the discharge current, voltage, and energy absorption. Schoene et al. [21] studied the response of different configured distribution lines to direct lightning on the top phase conductor, including the status of the arrester, the operation of the arrester disconnector, and the

* Corresponding author.

E-mail address: wjg@whu.edu.cn (J. Wang).

current in different places. The distribution of current was studied in [22]. Other direct lightning studies focus on simulation and calculation. Recent developments in this area can be found in [23–25].

Despite induced voltage experiments and relatively few direct lightning experiments, the induced voltage on the distribution line caused by direct lightning, especially on the parallel line has not been studied, which is of great importance to the protection of the double circuit distribution line. Also, considering double circuit configuration is common in both distribution lines and transmission lines, the research is very meaningful. This paper will make a supplement to this aspect.

2. Experiment and data

2.1. Experiment

Conghua is a mountainous area with frequent thunderstorms in southern China, where a 10 kV double circuit parallel distribution line for triggered lightning was built in 2018. Fig. 1 shows the layout of the line. From pole 1 to pole 17, the line is double circuit. After pole 17, circuit I turns left and ends at pole 22 due to space limitation. The line between pole 4 and pole 14, and between pole 18 and pole 21 is omitted, indicated by dotted lines. The interval between each pole is 70 m. Circuit I is 1513 m and circuit II is 1122 m. At both ends of circuit I, 10 kV distribution transformers are installed. Capacitances at the ends of circuit II are installed to equivalent to transformers at the ends of circuit I. Since the direct lightning current withstand level for distribution lines without arresters is relatively low, the arresters with series gap are installed on each pole of circuit I to protect the distribution line and gapless metal oxide arresters are installed at the ends of circuit I and circuit II to prevent lightning overvoltage from invading the distribution transformers. Circuit I was installed with ground wire, grounded at each pole. The grounding resistance is from 3.1 Ω to 22.0 Ω. The soil resistivity is between 180 Ω·m and 200 Ω·m.

The arrangement of three phases is vertical. The wire of phase C is 10 m above the ground and the interval between phases is 0.9 m. As shown in Fig. 1, the ground wire is marked in blue line, 1 m above phase A. The distance between two circuits is 2.5 m.

The lightning was triggered by a small rocket with copper wire at its

bottom. The lightning current was injected into phase A or phase C between pole 14 and pole 15 in circuit I. In the yellow box, there were an electrical-optical converter and coaxial shunt used to measure lightning current. Details of voltage measurement can be found in [26]. The system's sampling rate is 10 MS/s. Observation stations include pole 4 (S2), pole 16 (S9) on circuit II and pole 15 (S8) on circuit I. Here we mainly reveal the waveform characteristics at S2 and S9 on circuit II.

2.2. Data

There were 2 flashes recorded at 11:50 on June 26 and 12:18 on June 29, 2018, named as F1806261150 and F1806291218 respectively. F1806261150 contains 1 return stroke, while F1806291218 contains 14 return strokes. For F1806261150, the lightning directly struck on phase C, while for F1806291218, it struck on phase A.

For F1806291218, there was no current data recorded because the instrument was untriggered. However, the amplitude of the current is deduced according to the relation between it and the peak of electric field. The estimation error is 8% on average. More calculation details can be found in [28]. Here we show the voltage at two stations, S2 and S9. Return strokes recorded at S2 were intact while the 8th and 9th return strokes were not recorded at S9, meaning there were 12 return strokes at S9. The experimental data is shown in Table 1. In Fig. 2, the waveform of current in F1806261150 is shown. This flash has only one return stroke, and the lightning current has a negative polarity, with a

Table 1
Experimental data.

Lightning event	Direct struck phase	Peak value of return stroke current(kA)	10%–90% rise time of return stroke current (μs)	Number of return strokes recorded	
				S2	S9
F1806261150	C	8.3	0.4	1	1
F1806291218	A	16.6, 15.3, 11.5, 9.2, 8.9, 10.7, 10.5, 26.7, 8.2, 16.5, 12.9, 12.4, 17.7, 18.1	\	14	12

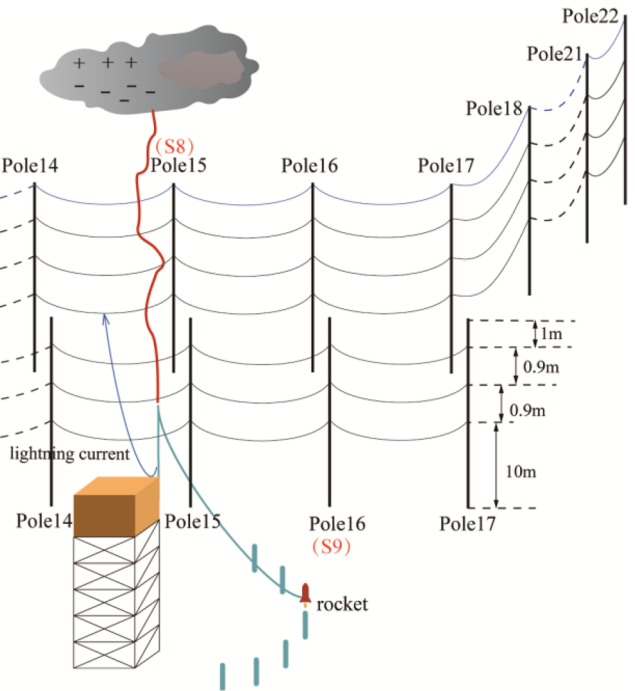
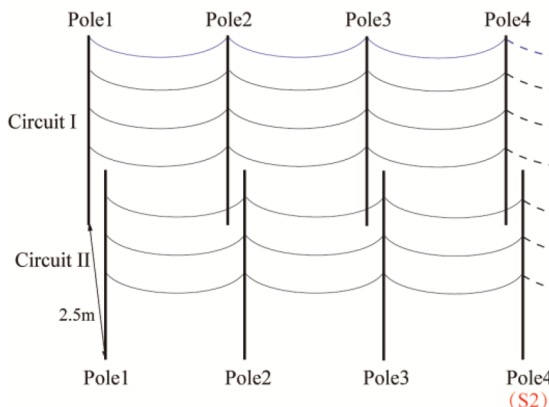


Fig. 1. The orientation of the double circuit distribution line and the rocket triggered lightning device.

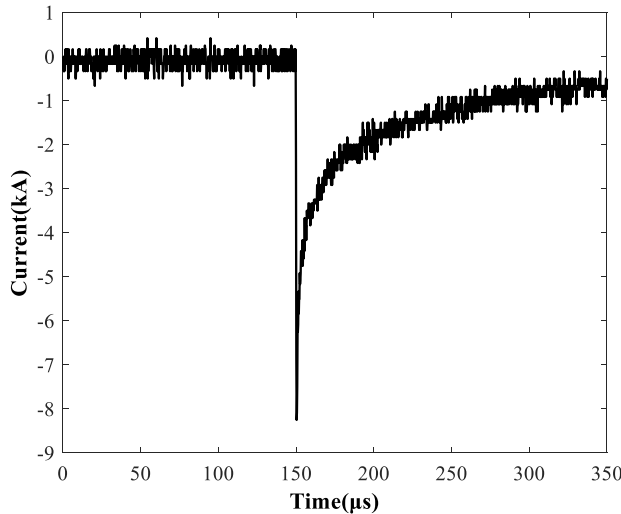


Fig. 2. Current waveform of F1806261150.

typical exponential waveform. The rise time of the negative peak is 0.4 μ s.

3. Results and analysis

3.1. Induced voltage on circuit II for F1806261150

The voltage at S2 and S9 for F1806261150 are overlapped, as shown in Fig. 3. It is obvious that the waveforms of three phases in two stations are similar. The voltage waveforms drop to their negative peak in a short time corresponding to leader development, and then experience a swift to a positive value corresponding to return stroke stage. Finally, they move into a duration of oscillation, continuing about 150 μ s. Since the line is open-ended and not matched-terminated, the lightning current injected by direct lightning reflects on the line through the grounding electrode of the surge arrester on the end pole, thus causing the oscillation waveforms in Fig. 3. During this period, the voltage reaches its positive peak. However, phase C voltage at S9 has a much larger negative peak compared with that at S2. Since S9 is the closest pole to the lightning point in circuit I, its negative peak is larger than that at S2.

There are three aspects influencing the voltage on the line. The first one is the induction field generated by the lightning channel, which is related to the height of the line. The second one is the coupling between the lightning conductor and the double circuit line, and the third one is the weakening effect of shielding wire on the voltage. When the lightning strikes on phase C in circuit I, the first factor makes the phase C voltage the lowest of the three phases. The remaining factors make

phase C voltage the largest of the three phases. Combining the effects of all factors, the amplitude of phase C voltage is the largest.

To better analyze the voltage, five parameters are defined, as shown in Fig. 4. They are the negative peak value V1, positive peak value V2, 10%–90% rise time of the negative peak T1, negative to positive peak transition time T2 and oscillation interval T3. Discrete Fourier Transform for the frequency spectrum analysis is used. Log coordinate is used for y axis to better present the resonances at higher frequencies, as shown in Fig. 5. The parameters are listed in Table 2.

As can be seen from Table 2, the negative peak value of phase C voltage at S9 was -54.7 kV, about 4 times larger than that of phase A and phase B at S9 and three-phase voltage at S2. The average value of the positive peak is 11.5 kV. For both stations, the rise time shows the regulation of phase B > phase A > phase C. The rise time of phase B is as large as around 130 μ s, which is much larger than those measured in [27]. The arithmetic mean of oscillation interval is 9.3 μ s. However, in [26], the oscillation interval is about two times that of ours. It is related to the length difference. Assuming an ideal speed of light for the calculation of wave reflection frequency on the line Circuit II, i.e., $f = 3 \times 10^8 / (2 \times 1122) = 133.69$ kHz. Note that according to [29], when considering the lossy ground, the transient line impedance due to the lossy line is frequency-dependent, which brings more high-frequency attenuation, and then the equivalent EM wave speed along the line is lower than the ideal light speed. Thus, the more reasonable frequency of the wave reflection for analysis would be smaller than 133.69 kHz. Compared with the observed 107.4 kHz (Fig. 5a) and 105.6 kHz (Fig. 5b) and a theoretical analyzed value of less than 133.69 kHz, this

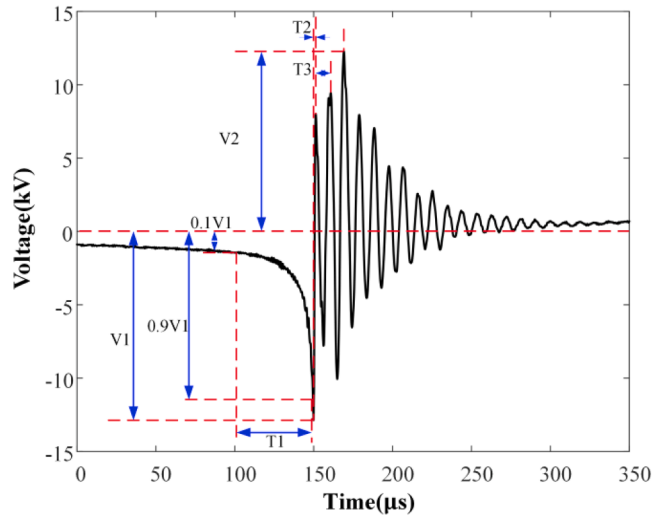


Fig. 4. Parameter definition of the voltage waveforms for F1806261150.

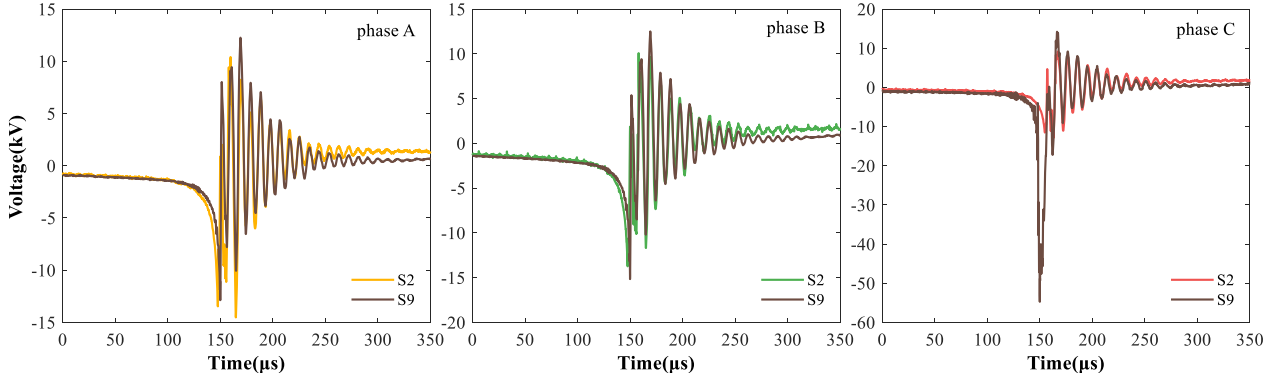


Fig. 3. Overlapping waveforms of three-phase overvoltage at S2 and S9 for F1806261150.

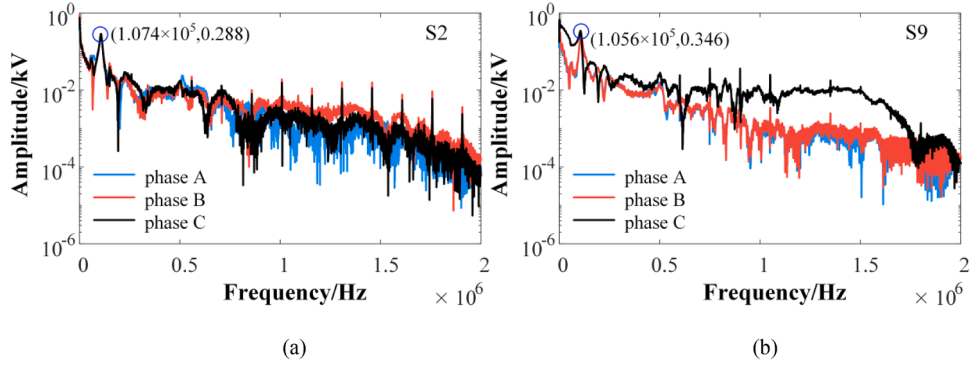


Fig. 5. Frequency spectrum analysis of three-phase voltage corresponding to F1806261150. (a). Frequency spectrum analysis of three-phase voltage at S2. (b). Frequency spectrum analysis of three-phase voltage at S9.

Table 2
Parameters of the voltage for F1806261150.

Parameters	S2			S9		
	A	B	C	A	B	C
Negative peak value (kV)	-14.5	-13.7	-12.9	-12.9	-15.2	-54.7
Positive peak value (kV)	10.4	10.1	9.2	12.3	12.5	14.2
10–90% rise time (μs)	55.9	132.4	45.4	68.1	130.0	7.6
Peak transition time (μs)	2.3	2.3	2.3	1.3	1.3	7.2
Average oscillation interval (μs)	9.3	9.3	9.3	9.3	9.3	9.5

explanation is reasonable. As for other resonances visible at higher frequencies, it is observed that the signal-noise ratio is quite high when comparing the amplitude of the single pulse with the frequency component nearby. On the other hand, the amplitude of each resonance pulse is much lower than the main lightning frequency component. We think that the resonances at higher frequencies would be related to the measuring systems or the non-linear electric equipment, such as the voltage divider and the transformer at the line terminations.

3.2. Induced voltage at S9 on circuit II for F1806291218

For F1806291218, artificial triggered lightning directly struck on phase A between pole 14 and pole 15 in circuit I. There were 12 return strokes recorded at S9 and the lightning current was between -8.9 kA and -18.1 kA. Since the overvoltage waveforms of 12 return strokes at S9 are similar, they are overlapped with their negative peak aligned, as shown in Fig. 6. With the color being deeper, the voltage corresponds to a larger return stroke current. The three-phase overvoltage at S9 has two characteristics. The first one is for different return strokes in a certain phase, the overvoltage waveforms are very similar. The second one is that the overvoltage waveforms of phase A and phase B are similar. However, the voltage of phase C is quite different. It features three negative pulses and a prominent positive pulse. This can be explained by the coupling mechanism between the waveforms at S8 in circuit I and the waveforms at S9 in circuit II. Here we exhibit phase C voltage waveforms at S8 and S9 corresponding to a current of -18.1 kA in Fig. 7. They are overlapped with their negative peaks aligned. It is clear in Fig. 7 that the prominent positive pulse in phase C voltage at S9 is similar to that at S8.

In Fig. 6(a) and (b), the voltage waveforms corresponding to current of -16.5 kA and -18.1 kA are different from others, with their wave tail rising again at about 150 μs. This is due to the coupling mechanism between circuit I and circuit II. The waveforms of these two return strokes at S8 in circuit I, the closest station to S9, and S9 at circuit II are overlapped at the negative peak, as shown in Fig. 8. The waveforms also

overlap at the wave tail. The rise at the wave tail of voltage at S9, 66 μs after the negative peak, is obviously due to the coupling of the voltage at S8. For these two return strokes, the voltage at S8 is a typical residual waveform, indicating the operation of the arrester. It has a relatively short valve action time, continuing about 45 μs. In Fig. 8(a), the voltage waveforms at S8 are truncated to -50 kV due to the voltage limitation of the secondary voltage divider.

The parameter definitions of phase A and phase B waveforms at S9 are the same with those in Fig. 4. For phase C waveform at S9, its parameter definitions are shown in Fig. 9. There are totally 8 parameters defined, including top three negative pulses V1, V3, V5, top three positive pulses V2, V4, V6, and time intervals T1, T2, and T3.

Parameters of three-phase overvoltage are shown in Fig. 10. The negative peak values of voltage of phase A and phase B are close, ranging from -11.7 kV to -25.7 kV, while the negative peak value of phase C voltage is larger, between -27.1 kV and -65.2 kV. The positive peak value of phase A in most cases is from 5 kV to 15 kV and for phase B, it is from 10 kV to 20 kV. Positive peak values exceeding 25 kV all occur in phase C voltage. The 10–90% rise time is between 20 μs and 60 μs in over half cases. The longest rise time can be over 100 μs in phase B, which is not seen in other two phases. For phase C, its rise time gathers around 20 μs, much smaller than phase A and phase B. This can be explained by the obvious waveform difference between phase C and the other two phases. For the negative to positive transition time, it is smaller than 3.0 μs and most of it gathers around 1 μs. This value for phase C is smaller than the other two phases. In terms of average oscillation interval, it is between 9.2 μs and 9.5 μs in all return strokes.

On the one hand, the induction field generated by the lightning channel will induce voltage on the line. On the other hand, there is a coupling between the lightning channel and the double circuit line. When lightning strikes on phase A conductor of circuit I, the coupling between phase C of circuit II and phase A of circuit I is the weakest, and the induction field is also the weakest since it is the lowest phase, but the phase C conductor is farthest from shielding wire and the weakening effect of shielding wire on phase C is also the lowest. The weakening effect of shielding wire plays a more important role in determining the amplitude of voltage, so phase C voltage is still the largest in this flash.

The three negative pulses and positive pulses of phase C are shown in Fig. 11. The negative pulses are all of negative values, however, some of positive pulses are also of negative values. The first negative pulse V1 has a large range, from -14.0 kV to -65.2 kV, and for V3 and V5, their ranges are relatively narrow. In some cases, V1 is smaller than V3 in its absolute value, while V3 is always larger than V5 in its absolute value. For the top three positive pulses, V2 is larger than V4 in 11 return strokes, while V6 is always larger than V4. The first positive pulse is from -25.1 kV to 35.7 kV. The second positive pulse V4 is around -8 kV in most return strokes and V6 is from -9.7 kV to 13.5 kV.

There is a good linear relation between the negative peak of three-phase voltage and the peak value of current, with the correlation

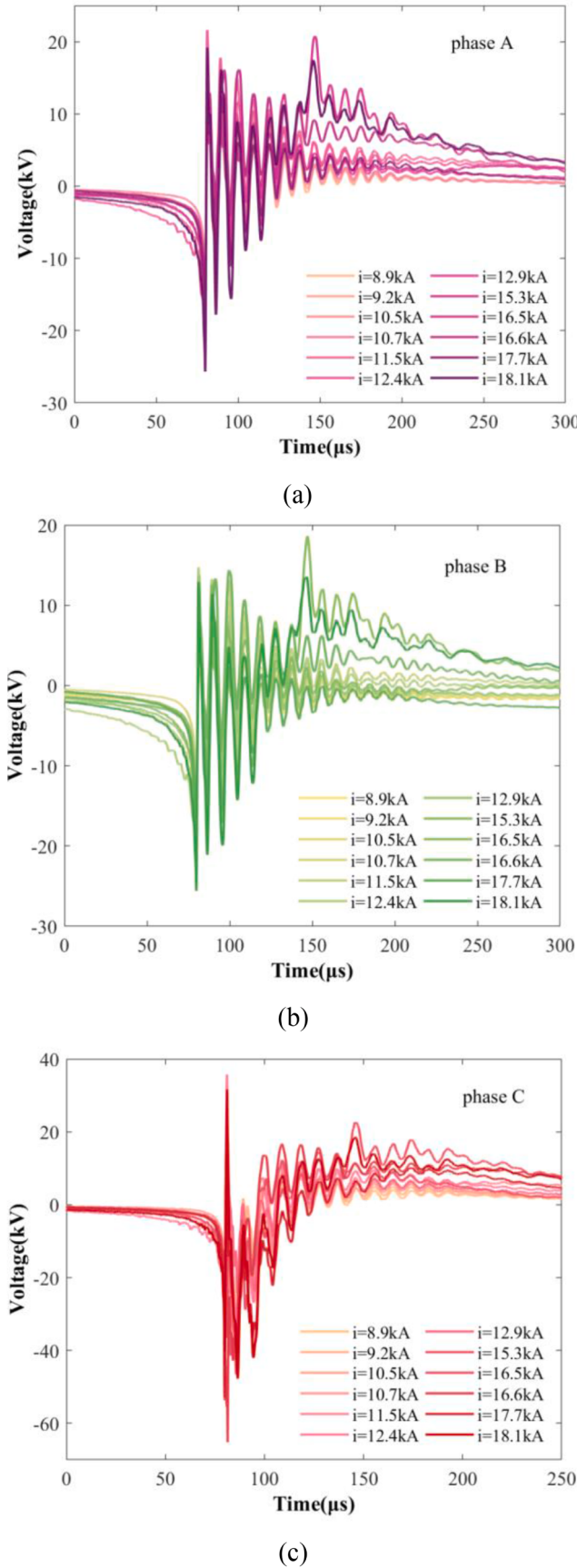


Fig. 6. Three-phase overvoltage at S9 corresponding to F1806291218. (a) Overvoltage of phase A. (b) Overvoltage of phase B. (c) Overvoltage of phase C.

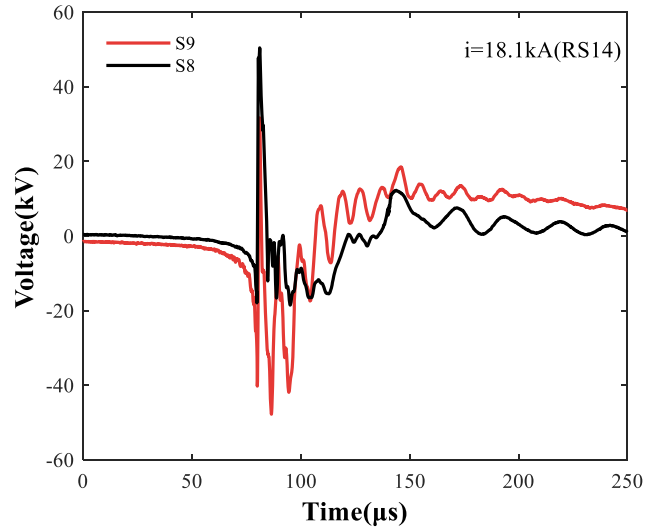


Fig. 7. Overlapping waveforms of phase C voltage at S8 and S9 corresponding to RS14 in F1806291218.

coefficient being 0.84, 0.86 and 0.86 for phase A, phase B, and the first negative pulse of phase C. Besides, the second positive pulse of phase C voltage also has a linear relation with that of the peak value of the current, with the correlation coefficient being 0.62.

3.3. Induced voltage at S2 on circuit II for F1806291218

There are 14 return strokes recorded at S2 for F1806291218. The three-phase voltage waveforms at S2 are similar and the waveforms of phase C are overlapped with their negative peak aligned, as shown in Fig. 12. It shows a typical induced voltage waveform, except for the second positive pulse larger than the first positive pulse in most cases. The parameter definitions are the same as those in Fig. 4 and the statistical results are shown in Fig. 13.

For three phases, most of the absolute values of negative peak are smaller than 30 kV. The average values of negative peak for phase A, phase B and phase C voltage are -21.7 kV, -20.7 kV and -19.3 kV. In over 50% return strokes in F1806291218, the positive peak value is smaller than 14 kV. The maximum value does not exceed 25 kV. Obviously, the positive peak value of phase A has a wider range than those of the other two phases. For 10–90% rise time of three-phase voltage, most of it ranges from 20 μs to 40 μs, while in the 12th return stroke, the rise time of phase B exceeds 100 μs. This parameter for phase C has a smaller range than the other two phases. The transition time of three-phase voltage is from 2 μs to 6 μs. The average oscillation interval is around 9.4 μs for three-phase voltage.

There is a good linear relation between the peak value of lightning current and the negative peak of voltage. The correlation coefficients for phase A, phase B, and phase C are 0.76, 0.70, and 0.77.

4. Discussion

Difference between the voltage on two stations of the distribution line as well as different struck phases will be discussed here. Table 3 listed the average values of parameters concerning negative peak value, positive peak value as well as the negative peak rise time. No matter which phase the lightning struck on, the absolute negative peak at S2 shows the regulation of $VA > VB > VC$ (VA means phase A voltage and the same can be explained for VB and VC), while the absolute negative peak at S9 shows the regulation of $VC > VB > VA$. The same rule can be applied to the positive peak value at S2 and S9 when the lightning struck phase C, while it is a bit different for the case in which the lightning struck on phase A. It was $VA > VC > VB$ at S2, while it was $VC > VA > VB$

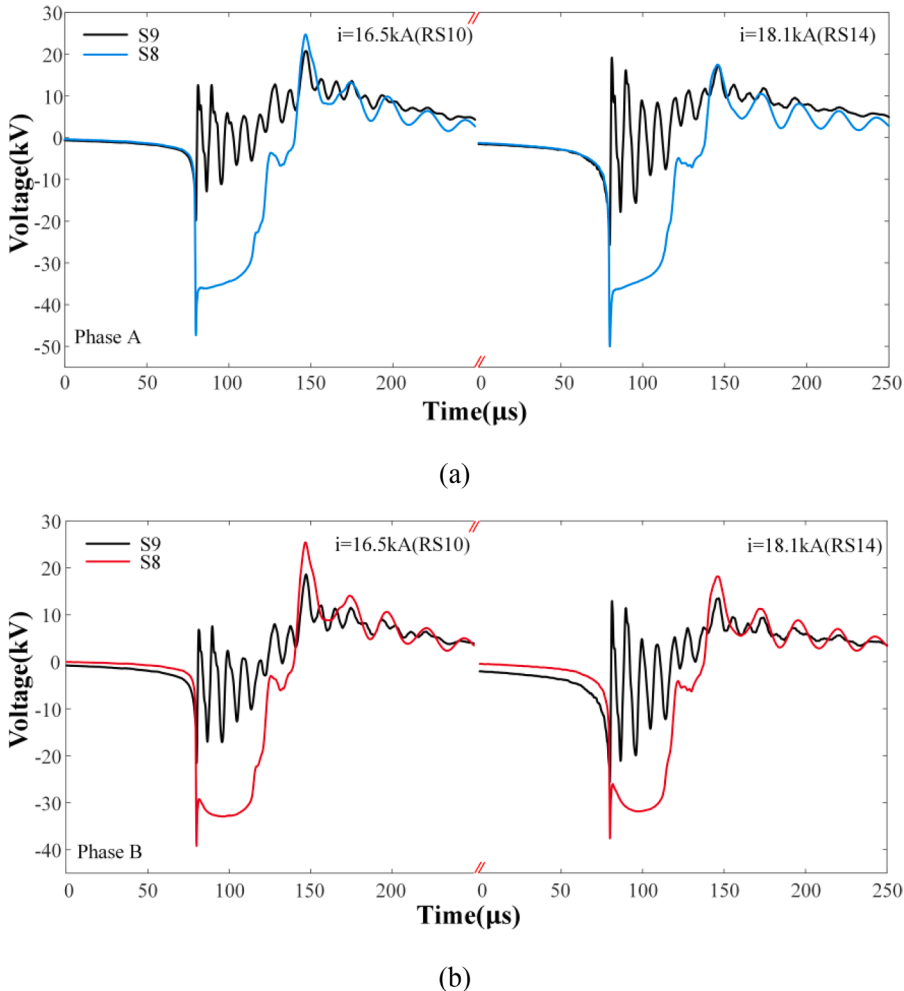


Fig. 8. Overlapping waveforms of voltage at S8 and S9 corresponding to RS10 and RS14 in F1806291218. (a) Overvoltage of phase A. (b) Overvoltage of phase B.

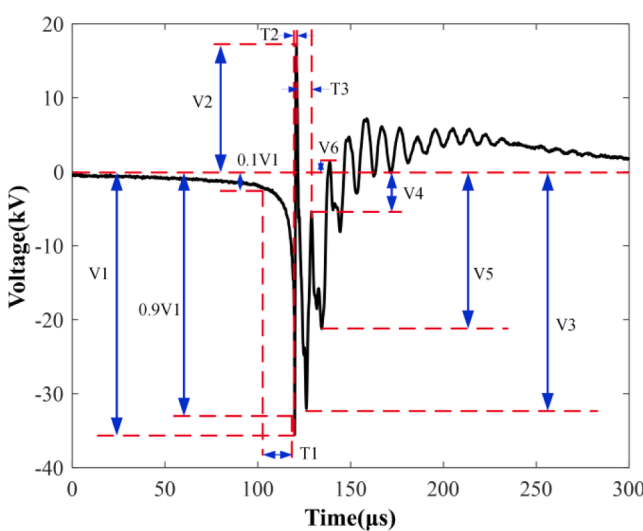


Fig. 9. Parameter definitions of the waveform of phase C voltage for F1806291218.

at S9. For rise time, all cases show TB > TA > TC. (TA means time for phase A and the same can be explained for TB and TC.)

It can be found that at the same station, no matter which phase the lightning struck on, it has no obvious effect on the voltage, however, it is

worth noting that when the lightning struck on phase C, the rise time of voltage in each phase, especially in phase B, is much larger than that when the lightning struck on phase A. For instance, in Table 2, when the direct struck phase was phase C, the negative peak rise time for phase A, B and C at S2 are 55.9 μs, 132.4 μs, and 45.4 μs. When the struck phase was phase A, those values at S2 are 30.1 μs, 51.6 μs, and 28.1 μs respectively. Both at S2 and S9, the rise time of phase B can be over 130 μs when the lightning struck phase C, which is very scarce in [26].

Considering the voltage at S2 and S9, in most cases the negative peak values of phase A and phase B at S2 are larger than those at S9, while the negative peak value of phase C at S9 is much larger than that at S2. For lightning on phase C, the absolute average values of the negative peak of phase C at S2 and S9 are 12.9 kV and 54.7 kV respectively and for lightning on phase A, the above values are 19.3 kV and 37.5 kV. The negative peak value of phase C at S9 is 2.5 times that of S2, and the maximum can reach 4.3 times. Besides, the negative peak values of three-phase voltage at S2 are quite similar, with a difference smaller than 10 kV. The rise time of voltage of phase C at S9 is shorter than that at S2, with the average values being 15.1 μs and 28.1 μs for lightning in phase A and being 7.6 μs and 45.4 μs for lightning in phase C.

For F1806261150, the lightning current is -8.3 kA. The negative peak value of overvoltage at S2 is from -12.9 kV to -14.5 kV, and that at S9 is from -12.9 kV to -54.7 kV. For F1806291218, the negative peak of induced voltage at S9 was between -11.7 kV and -65.2 kV corresponding to lightning current from -8.2 kA to -18.1 kA. At S2, the induced voltage is from -10.5 kV to -42.8 kV corresponding to lightning current from -8.2 kA to -26.7 kA. At the ends of circuit II, arresters without gaps are

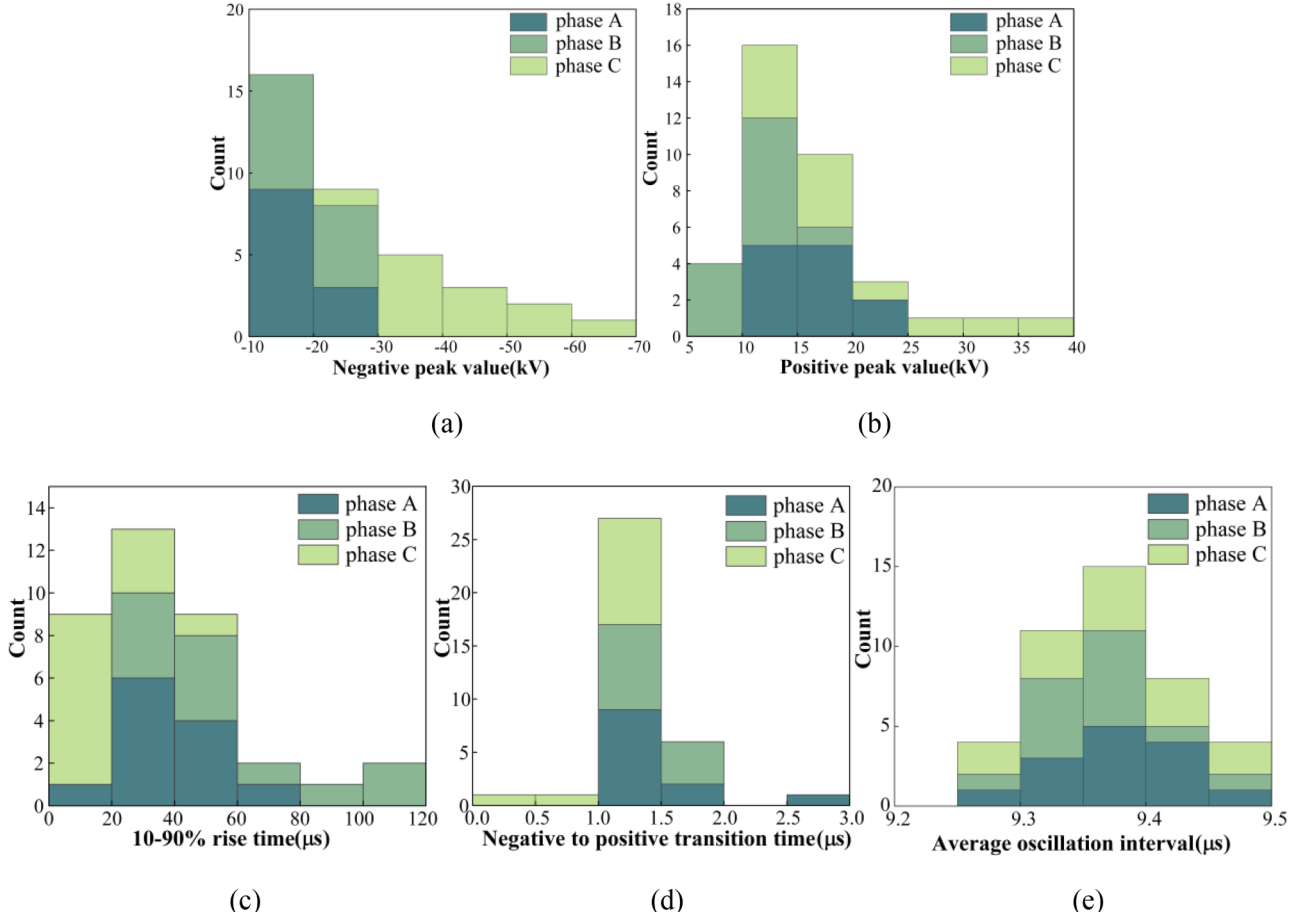


Fig. 10. Parameters for three-phase voltage at S9 corresponding to F1806291218. (a). Negative peak value of three-phase voltage. (b). Positive peak value of three-phase voltage. (c). Negative 10–90% rise time of three-phase voltage. (d). Negative to positive transition time of three-phase voltage. (e). Average oscillation interval of three-phase voltage.

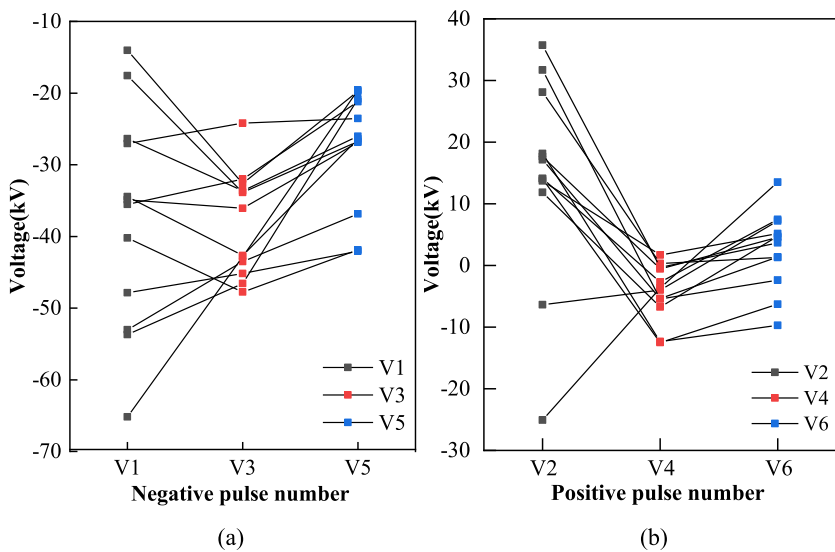


Fig. 11. The negative pulses and positive pulses of phase C voltage in F1806291218 at S9. (a). The value of negative pulses V1, V3 and V5. (b). The value of positive pulses V2, V4 and V6.

installed. The 50% impulse flashover voltage of the insulator is 240 kV for positive polarity and -296.4 kV for negative polarity, so there is no flashover in these two flashes.

5. Conclusion

The induced voltage on the distribution line caused by direct lightning on a parallel line is of great importance to the protection of double

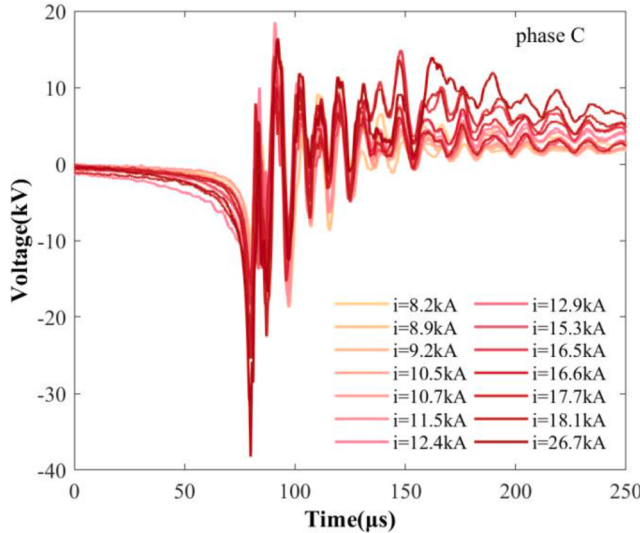


Fig. 12. The waveforms of phase C at S2 corresponding to F1806291218.

circuit distribution line. In this paper, triggered lightning was applied to strike a 10 kV double circuit distribution line on different phases.

For event F1806261150 containing 1 return stroke, the lightning struck on phase C. The three-phase overvoltage waveforms all show the characteristics of fast dropping to negative peak, swift polarity transition, and the final oscillation. Phase C voltage at S9 is much larger than that at S2 and the negative peak value of phase C voltage at S9 is much larger than the other two phases, being -54.7 kV.

For event F1806291218, the lightning struck on phase A with 14 return strokes. At S9, phase C voltage is obviously different, featuring three obvious negative pulses and one prominent positive pulse. The negative peak value of three-phase overvoltage ranges from -11.7 kV to -65.2 kV corresponding to lightning current from -8.2 kA to -18.1 kA. Compared with the negative peak, the positive peak value is smaller at two stations.

No matter which phase the lightning struck in these two flashes, phase C voltage at S9 is always the largest. Considering the line layout and other factors, it deserves more investigations by simulation to reveal deeper mechanism of the waveforms in the future.

Table 3
Average values of parameters of two flashes.

Station	Direct struck phase	Phase	Absolute value of negative peak (kV)	Positive peak value (kV)	Negative peak rise time (μs)
S2	C	A	14.5	10.4	55.9
		B	13.7	10.1	132.4
		C	12.9	9.2	45.4
	A	A	21.7	14.8	30.1
		B	20.7	9.4	51.6
		C	19.3	13.2	28.1
	C	A	12.9	12.3	68.1
		B	15.2	12.5	130.0
		C	54.7	14.2	7.6
	A	A	17.7	16.3	37.3
		B	19.1	12.4	57.2
		C	37.5	18.6	15.1

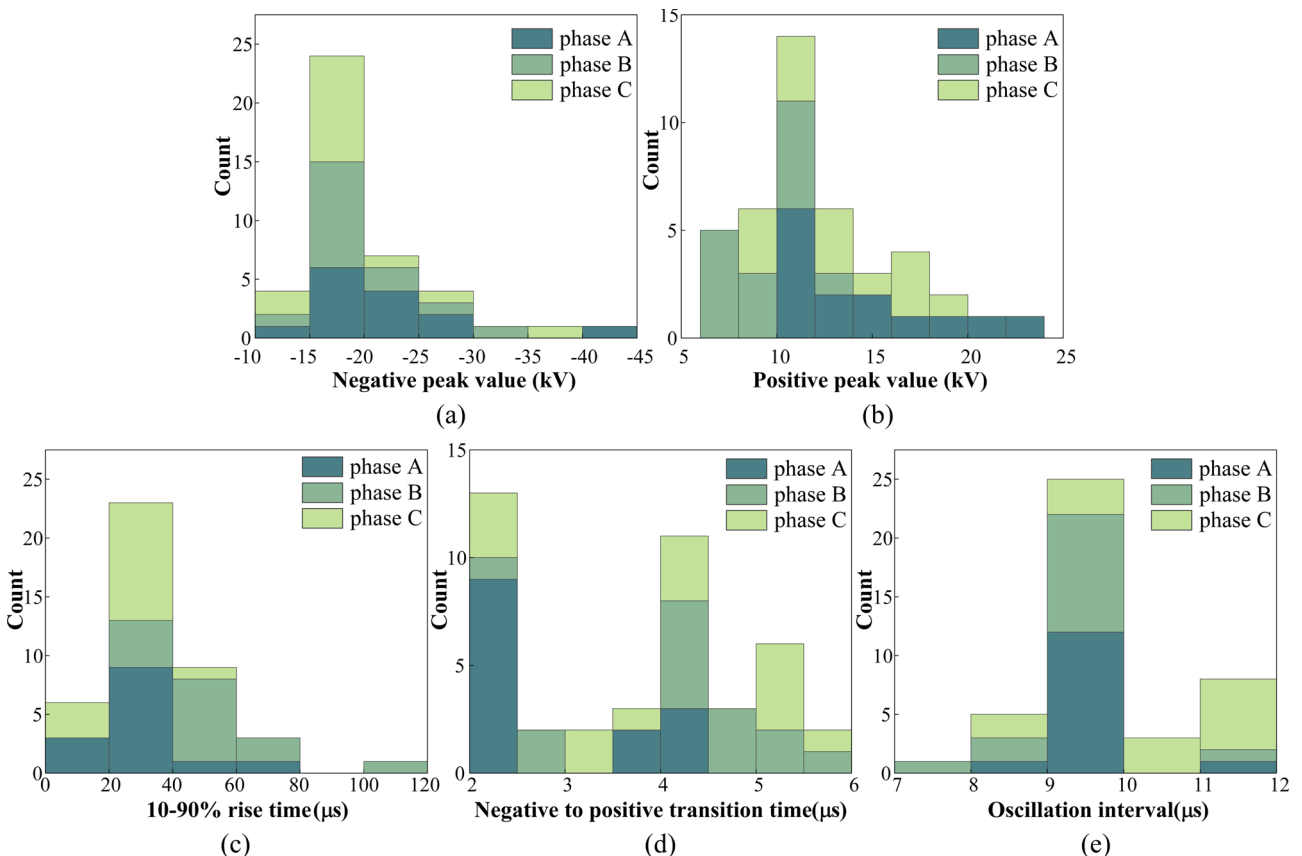


Fig. 13. Parameters for three-phase voltage at S2 corresponding to F1806291218. (a) Negative peak value of three-phase voltage. (b) Positive peak value of three-phase voltage. (c) Negative 10–90% rise time of three-phase voltage. (d) Negative to positive transition time of three-phase voltage. (e) Average oscillation interval of three-phase voltage.

CRediT authorship contribution statement

Yating Zhao: Conceptualization, Methodology, Software, Writing – original draft, Writing – review & editing, Visualization, Formal analysis. **Jianguo Wang:** Validation, Writing – review & editing, Supervision, Project administration, Data curation, Resources, Formal analysis. **Li Cai:** Formal analysis, Writing – review & editing, Supervision, Project administration, Funding acquisition, Investigation. **Quanxin Li:** Data curation. **Mi Zhou:** Project administration. **Rui Su:** Software. **Zhilong Xu:** Software. **Yadong Fan:** Resources.

Declaration of Competing Interest

The authors declare that they have no known competing financial interests or personal relationships that could have appeared to influence the work reported in this paper.

Acknowledgement

The work of this paper was supported by the National Natural Science Foundation of China under Grant No. 51807144. The authors want to express their gratitude to all the staff at Guangdong Electric Power Research Institute and Guangzhou Field Experiment Site for Lightning Research and Testing (GFESLRT).

References

- [1] S. Oguchi, T. Ishii, S. Okabe, Y. Sakamoto, M. Tsuji, A. Asakawa, Observational and experimental study of the lightning stroke attraction effect with ground wire system constructions, *IEEE Trans. Dielectr. Electr. Insul.* 19 (1) (2012) 363–370. February.
- [2] H. Chen, Y. Du, M. Yuan, Q.H. Liu, Lightning-induced voltages on a distribution line with surge arresters using a hybrid FDTD–SPICE method, *IEEE Trans. Power Delivery* 33 (5) (2018) 2354–2363. Oct.
- [3] R. Araneo, A. Andreotti, J. Brandão Faria, S. Celozzi, D. Assante, L. Verolino, Utilization of underbuilt shield wires to improve the lightning performance of overhead distribution lines hit by direct strokes, *IEEE Trans. Power Delivery* 35 (4) (2020) 1656–1666. Aug.
- [4] F. de la Rosa, R. Valdivia, H. Perez, J. Loza, Discussion about the inducing effects of lightning in an experimental power distribution line in Mexico, *IEEE Trans. Power Delivery* 3 (3) (1988) 1080–1089. July.
- [5] T.A. Short, R.H. Ammon, Monitoring results of the effectiveness of surge arrester spacings on distribution line protection, *IEEE Trans. Power Delivery* 14 (3) (1999) 1142–1150. July.
- [6] T. Miyazaki, S. Okabe, A detailed field study of lightning stroke effects on distribution lines, *IEEE Trans. Power Delivery* 24 (1) (2009) 352–359. Jan.
- [7] L. Cai, J. Wang, M. Zhou, S. Chen, J. Xue, Observation of natural lightning-induced voltage on overhead power lines, *IEEE Trans. Power Delivery* 27 (4) (2012) 2350–2359. Oct.
- [8] A.J. Eriksson, D.V. Meal, Lightning performance and overvoltage surge studies on a rural distribution line[J], *IEE Proc. C Gener. Transm. Distrib.* 129 (2) (1982) 59.
- [9] J. Takami, S. Okabe, Characteristics of direct lightning strokes to phase conductors of UHV transmission lines, *IEEE Trans. Power Delivery* 22 (1) (2007) 537–546. Jan.
- [10] Kazuo Nakada, Tsutomu Yokota, Shigeru Yokoyama, Akira Asakawa, Tetsuji Kawabata, Effect of overhead ground wires on reduction of failure rates of surge arresters on power distribution lines, *IEEJ Trans. Power Energy* 117 (6) (1997) 857–863.
- [11] S. Yokoyama, A. Asakawa, Experimental study of response of power distribution lines to direct lightning hits, *IEEE Trans. Power Delivery* 4 (4) (1989) 2242–2248. Oct.
- [12] A. Piantini, J.M. Janiszewski, A. Borghetti, C.A. Nucci, M. Paolone, A scale model for the study of the LEMP response of complex power distribution networks, *IEEE Trans. Power Delivery* 22 (1) (2007) 710–720. Jan.
- [13] S. Yokoyama, K. Yamamoto, H. Kinoshita, Analogue simulation of lightning induced voltages and its application for analysis of overhead-ground-wire effects [J], *IEE Proc. C Gener. Transm. Distrib.* 132 (4) (2008) 208–216.
- [14] Y. Imai, H. Tsuchihashi, A. Asakawa, Experimental analysis of lightning overvoltages induced on low-voltage distribution lines[J], *Electr. Eng. Jpn.* 111 (5) (2010) 72–82.
- [15] M.M. Newman, J.R. Stahmann, J.D. Robb, E.A. Lewis, S.G. Martin, S.V. Zinn, Triggered lightning strokes at very close range, *J. Geophys. Res.* 72 (18) (1967) 4761–4764.
- [16] P.P. Barker, T.A. Short, A.R. Eybert-Berard, J.P. Berlandis, Induced voltage measurements on an experimental distribution line during nearby rocket triggered lightning flashes, *IEEE Trans. Power Delivery* 11 (2) (1996) 980–995. April.
- [17] M. Rubinstein, M.A. Uman, P.J. Medelius, E.M. Thomson, Measurements of the voltage induced on an overhead power line 20m from triggered lightning, *IEEE Trans. Electromagn. Compat.* 36 (2) (1994) 134–140. May.
- [18] Y. Matsumoto, et al., Measurement of lightning surges on test transmission line equipped with arresters struck by natural and triggered lightning, *IEEE Trans. Power Delivery* 11 (2) (1996) 996–1002. April.
- [19] H. Motoyama, K. Shinjo, Y. Matsumoto, N. Itamoto, Observation and analysis of multiphase back flashover on the Okushishiku Test Transmission Line caused by winter lightning, *IEEE Trans. Power Delivery* 13 (4) (1998) 1391–1398. Oct.
- [20] M.I. Fernandez, K.J. Rambo, V.A. Rakov, M.A. Uman, Performance of MOV arresters during very close, direct lightning strikes to a power distribution system, *IEEE Trans. Power Delivery* 14 (2) (1999) 411–418. April.
- [21] J. Schoene, et al., Direct lightning strikes to test power distribution lines—Part I: experiment and overall results, *IEEE Trans. Power Delivery* 22 (4) (2007) 2236–2244. Oct.
- [22] B.A. DeCarlo, et al., Distribution of currents in the lightning protective system of a residential building—part I: triggered-lightning experiments, *IEEE Trans. Power Delivery* 23 (4) (2008) 2439–2446. Oct.
- [23] K. Ishimoto, F. Tossani, F. Napolitano, A. Borghetti, C.A. Nucci, Direct lightning performance of distribution lines with shield wire considering LEMP effect, *IEEE Trans. Power Delivery* 37 (1) (2022) 76–84. Feb.
- [24] R. Araneo, A. Andreotti, J. Brandão Faria, S. Celozzi, D. Assante, L. Verolino, Utilization of underbuilt shield wires to improve the lightning performance of overhead distribution lines hit by direct strokes, *IEEE Trans. Power Delivery* 35 (4) (2020) 1656–1666. Aug.
- [25] D.O. Belko and G.V. Podporkin, Analysis of current distribution among long-flashover arresters for 10kV overhead line protection against direct lightning strikes, 2016 33rd International Conference On Lightning Protection (ICLP), 2016, pp. 1–6.
- [26] J. Wang, et al., Observation of induced voltage at the terminal of 10kV distribution line by nearby triggered lightning, *IEEE Trans. Power Delivery* 35 (4) (2020) 1968–1976. Aug.
- [27] Y. Zhang, et al., Experiments on lightning protection for automatic weather stations using artificially triggered lightning, *IEEJ Trans. Electr. Electr. Eng.* 8 (4) (2013) 313–321.
- [28] Q. Li, J. Wang, L. Cai, M. Zhou, Y. Fan, On the return-stroke current estimation of Foshan Total Lightning Location System (FTLLS), *Atmos. Res.* 248 (2021), 105194.
- [29] F. Rachidi, C.A. Nucci, M. Ianoz, C. Mazzetti, Influence of a lossy ground on lightning-induced voltages on overhead lines, *IEEE Trans. Electromagn. Compat.* 38 (3) (1996) 250–264. Aug.